CAAI Transactions on Intelligence Technology

WILEY

ORIGINAL RESEARCH OPEN ACCESS

A Competitive Model via *k*WTA Network for Multi-Agent Systems Considering Noise and Communication Disturbances

Jiexing Li[1,2,3] | Shuai Li[2]

[1]College of Computer, Qinghai Normal University, Xining, China | [2]Faculty of Information Technology and Electrical Engineering, University of Oulu, Oulu, Finland | [3]Qinghai Provincial Key Laboratory of IoT, Qinghai Normal University, Xining, China

Correspondence: Shuai Li (shuai.li@oulu.fi)

Received: 13 June 2026 | **Revised:** 30 July 2026 | **Accepted:** 12 August 2026

Keywords: communication disturbances | consensus estimator | *k*-winners-take-all (WTA) problem | multi-agent system

ABSTRACT

The *k*-winners-take-all (*k*WTA) problem, as a competitive selection strategy, is crucial in multi-agent systems. However, existing noise-robust *k*WTA networks mainly address noise while overlooking communication disturbances. The coexistence of both factors significantly degrades solution accuracy and hinders distributed consensus estimation. To address these issues, this paper first proposes an accelerated-convergence and noise-tolerant *k*WTA (ACNT-*k*WTA) network by introducing a nonlinear activation function and an error-integral term. Second, a robust consensus estimator is developed and integrated with the proposed ACNT-*k*WTA network to construct an enhanced-robustness competitive coordination (ERCC) model, which simultaneously suppresses noise and communication disturbances. Theoretical analyses demonstrate the global convergence of the proposed ACNT-*k*WTA network and the robust consensus estimator. Ultimately, the effectiveness and superiority of the proposed model are demonstrated through comparative numerical simulations and physical experiments.

1 | Introduction

Multi-agent systems have recently attracted considerable research interest due to their capacity for solving problems beyond the reach of a single agent, leading to widespread deployment in fields such as unmanned aerial vehicles [1], swarm robotics [2], smart grids [3], multiple manipulators [4] and wireless sensor networks [5]. Fundamentally, the interactions among agents can be described as cooperative or competitive mechanisms. The cooperative mechanism enables agents to coordinate with each other to execute complex joint tasks, such as formation control [6] and cooperative transport [7]. The competitive mechanism, which inevitably arises due to resource constraints, is equally crucial in multi-agent systems [8]. Prevalent competitive mechanisms in multi-agent systems include game theory [9], market mechanism [10] and auction algorithm [11]. Besides these, the *k*WTA problem is also an effective competitive mechanism. By selecting k optimal agents as winners from n candidates, while designating the rest as losers, it is widely applied in various resource allocation scenarios [12, 13]. To facilitate the real-time resolution of such competitive selection, the *k*WTA problem is commonly case as a QP problem [14]. Reinforcement learning methods are not well-suited for solving the *k*WTA problem in multi-robot systems due to their reliance on massive data, high trial-and-error risks in dynamic environments. However, neurodynamic approaches, which originate from neural networks and dynamical systems

Abbreviations: ACNT-*k*WTA, accelerated-convergence and noise-tolerant *k*WTA; ERCC, enhanced-robustness competitive coordination; FB, Fischer–Burmeister; KKT, Karush–Kuhn–Tucker; *k*WTA, *k*-winners-take-all; QP, quadratic programming.

This is an open access article under the terms of the Creative Commons Attribution License, which permits use, distribution and reproduction in any medium, provided the original work is properly cited.

© 2026 The Author(s). *CAAI Transactions on Intelligence Technology* published by John Wiley & Sons Ltd on behalf of The Institution of Engineering and Technology and Chongqing University of Technology.

[15–18], are widely employed to solve optimization problems. When specifically applied to the *k*WTA problem, the resulting models are commonly referred to as *k*WTA networks.

When solving *k*WTA networks, it is inevitably subjected to various types of noise arising from measurement errors [19], truncation errors [20] and external perturbations [21]. These adverse effects will significantly compromise the solution accuracy of *k*WTA networks. A common approach is to rely on dedicated denoising hardware or front-end filters to suppress noise before the model is executed. However, this approach imposes a heavy computational burden and, more importantly, reduces the system's effectiveness when dealing with time-varying inputs. Consequently, an increasing number of *k*WTA networks are designed to mitigate the effect of noise. For example, a dual-based *k*WTA network that accounts for Gaussian noise is provided in [22], which establishes the theoretical conditions required for the network to maintain a high probability of correct competitive selection. Similarly, the performance of a *k*WTA network under multiplicative noise is evaluated in [23]. In addition, several gradient-based differential *k*WTA networks capable of resisting basic forms of noise are presented in [24, 25]. Furthermore, a *k*WTA network is presented in [26] to counteract complex polynomial noise by capturing its characteristics. In summary, these robust designs enable *k*WTA networks to maintain precision despite the presence of noise.

Moreover, due to the presence of the equality constraint, directly applying *k*WTA networks to multi-agent systems requires the collection of global information [27]. Therefore, consensus estimators are widely utilised to facilitate distributed implementations by enabling agents to estimate global states purely through local communication [28–30]. By incorporating consensus estimators, the aforementioned *k*WTA networks are successfully deployed in distributed multi-agent coordination tasks [24–26]. Existing studies mainly concern the consensus estimation problem under topological structures, such as weight-unbalanced topologies [31] and switching topologies [32]. Nevertheless, these studies remain restricted to ideal communication conditions. In practical applications, the information exchange among agents are inevitably influenced by communication disturbances, such as packet loss [33], sensor noise [34] and environmental fluctuations [35]. Meanwhile, *k*WTA networks are concurrently affected by noise. The coexistence of communication disturbances and noise will severely compromise the consensus performance and competitive decision-making of distributed multi-agent systems. Hence, there is a pressing need for a robust competitive coordination model that offers resilience against both noise and communication disturbances.

To overcome these issues, an accelerated-convergence and noise-tolerant *k*WTA (ACNT-*k*WTA) network is first developed in this paper. Specifically, a nonlinear activation function is incorporated to accelerate convergence significantly. Concurrently, by integrating an error-integral term, the noise within the network is effectively suppressed. Second, a robust consensus estimator is developed to enable distributed implementation while mitigating communication disturbances. By integrating the robust consensus estimator with the ACNT-*k*WTA network, an enhanced-robustness competitive coordination (ERCC) model is constructed. The efficacy and advantages of the proposed model are verified through comparative simulations against existing *k*WTA networks on multi-agent competitive coordination tasks. Finally, the practicality of the proposed ERCC model is corroborated by its deployment on E-puck robots in a mobile target tracking scenario. The overall framework of this paper is depicted in Figure 1, and the primary contributions are outlined as follows.

1. By incorporating a nonlinear activation function and an error-integral term, an ACNT-*k*WTA network is proposed to rapidly and accurately obtain optimal solutions under noisy conditions. Theoretical results confirm its global convergence and robustness.
2. A robust consensus estimator is proposed to resist communication disturbances. By integrating this estimator with the proposed ACNT-*k*WTA network, an ERCC model is

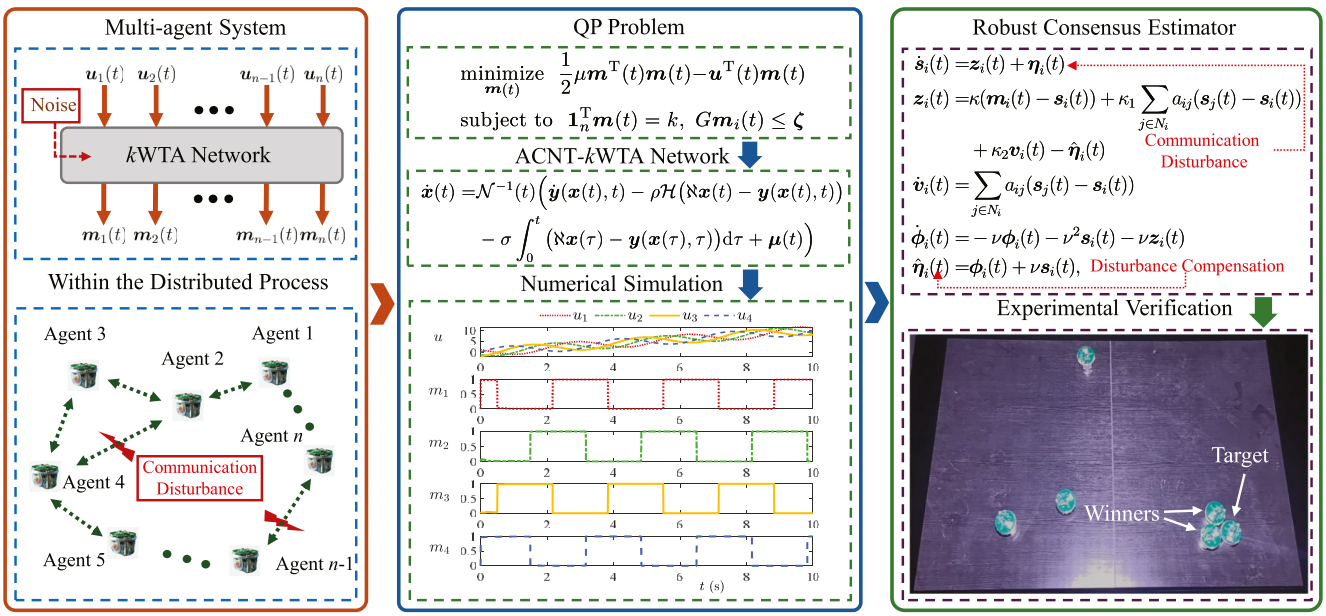


FIGURE 1 | Overall research framework of this paper.

constructed that, for the first time, simultaneously mitigates noise and communication disturbances.

The rest of this paper is structured as follows. Section 2 introduces the problem formulation, the design of the ACNT-k WTA network, and the construction of the ERCC model. Section 3 presents the theoretical analyses of convergence and robustness. Section 4 provides illustrative examples and results. Section 5 concludes this paper.

2 | Problem Formulation, Network Design and Model Construction

The kWTA problem is initially formulated as a constrained QP problem, which is then reformulated into a compact matrix equation using the KKT conditions and the FB function. Subsequently, the ACNT-kWTA network is designed to achieve accelerated convergence and noise tolerance. Finally, the ERCC model is established by incorporating the ACNT-kWTA network with a robust consensus estimator.

2.1 | Problem Formulation

The kWTA problem is a competitive selection mechanism that identifies the k optimal agents from a set of n candidates. Mathematically, it is formulated as:

$$\boldsymbol{m}_i(t) = \Upsilon(\boldsymbol{u}_i(t)) = \begin{cases} 1, & \text{if } \boldsymbol{u}_i(t) \in \mathbb{K} \\ 0, & \text{if } \boldsymbol{u}_i(t) \notin \mathbb{K}, \end{cases} \tag{1}$$

where $\boldsymbol{u}_i(t)$ is the ith input at time t, and $\boldsymbol{m}_i(t)$ is the corresponding output component; $\mathbb{K}$ denotes a set that consists of the k optimal agents from candidates $\boldsymbol{u}(t)$; $\Upsilon(\cdot)$ represents the selection function that implements the kWTA problem. It is worth noting that the above formulation merely provides an abstract mathematical description of the kWTA problem. Further, following the approach in [14], this problem is equivalently reformulated as the following constrained QP problem:

$$\underset{\boldsymbol{m}(t)}{\text{minimize}} \quad \frac{1}{2}\gamma \boldsymbol{m}^{\mathrm{T}}(t)\boldsymbol{m}(t) - \boldsymbol{u}^{\mathrm{T}}(t)\boldsymbol{m}(t) \tag{2a}$$

$$\text{subject to} \quad \boldsymbol{1}_n^{\mathrm{T}}\boldsymbol{m}(t) = k \tag{2b}$$

$$G\boldsymbol{m}_i(t) \le \boldsymbol{\zeta}, \tag{2c}$$

where $\gamma < (\boldsymbol{u}_k - \boldsymbol{u}_{k+1}) \in \mathbb{R}^+$ ensures a finite resolution of the QP problem, with $\boldsymbol{u}_k$ and $\boldsymbol{u}_{k+1}$ denoting the kth and $(k+1)$th largest components of inputs, respectively; superscript $(\cdot)^{\mathrm{T}}$ denotes the matrix transpose; $G \in \mathbb{R}^{2n\times n}$ is constructed as $G = [I_n; -I_n]$, with $I_n \in \mathbb{R}^{n\times n}$ denoting the n-dimensional identity matrix; $\boldsymbol{\zeta} = [\boldsymbol{1}_n; \boldsymbol{0}_n] \in \mathbb{R}^{2n}$, with $\boldsymbol{1}_n$ and $\boldsymbol{0}_n$ being n-dimensional all-one vector and all-zero vector, respectively.

To address the QP problem (2), Lagrange multipliers $\lambda(t) \in \mathbb{R}$ and $\boldsymbol{\epsilon}(t) \in \mathbb{R}^{2n}$ are introduced to handle equality constraint (2b) and inequality constraint (2c), respectively. The corresponding Lagrangian function is given as:

$$\begin{aligned} \mathcal{L}(\boldsymbol{m}(t), \lambda(t), \boldsymbol{\epsilon}(t)) &= \frac{1}{2}\gamma \boldsymbol{m}^{\mathrm{T}}(t)\boldsymbol{m}(t) - \boldsymbol{u}^{\mathrm{T}}(t)\boldsymbol{m}(t) \\ &+ \lambda^{\mathrm{T}}(t)\big(\boldsymbol{1}_n^{\mathrm{T}}\boldsymbol{m}(t) - k\big) + \boldsymbol{\epsilon}^{\mathrm{T}}(t)(G\boldsymbol{m}(t) - \boldsymbol{\zeta}). \end{aligned} \tag{3}$$

By applying the KKT conditions, the optimal solution $\boldsymbol{m}^*(t)$ and corresponding Lagrangian multipliers $\lambda^*(t)$ and $\boldsymbol{\epsilon}^*(t)$ are obtained. Accordingly, (2) is rewritten as:

$$\begin{cases} \gamma \boldsymbol{m}^*(t) - \boldsymbol{u}(t) + \boldsymbol{1}_n\lambda^*(t) + G^{\mathrm{T}}\boldsymbol{\epsilon}^*(t) = \boldsymbol{0} & \text{(4a)} \\ \boldsymbol{1}_n^{\mathrm{T}}\boldsymbol{m}(t) - k = 0 & \text{(4b)} \\ \boldsymbol{\epsilon}^*(t) \ge \boldsymbol{0}, \boldsymbol{\zeta} - G\boldsymbol{m}^*(t) \ge \boldsymbol{0} & \text{(4c)} \\ \boldsymbol{\epsilon}^{*\mathrm{T}}(t)(\boldsymbol{\zeta} - G\boldsymbol{m}(t)) = \boldsymbol{0}. & \text{(4d)} \end{cases}$$

Note that (4c) and (4d) constitute a complementarity system, which can be equivalently handled by leveraging the FB function, defined as $F_\iota(\boldsymbol{a}, \boldsymbol{b}) = \boldsymbol{a} + \boldsymbol{b} - \sqrt{\boldsymbol{a}\circ\boldsymbol{a} + \boldsymbol{b}\circ\boldsymbol{b} + \iota}$ where ι, $\boldsymbol{a}$ and $\boldsymbol{b} \in \mathbb{R}^n$ are vectors; $\circ$ denotes the Hadamard product. This function satisfies that $F_\iota(\boldsymbol{a}, \boldsymbol{b}) = \boldsymbol{0} \Leftrightarrow \boldsymbol{a} \ge \boldsymbol{0}, \boldsymbol{b} \ge \boldsymbol{0}$ and $\boldsymbol{a}^{\mathrm{T}}\boldsymbol{b} = \boldsymbol{0}$. Based on this property, (4) is reformulated as:

$$\begin{cases} \gamma \boldsymbol{m}^*(t) - \boldsymbol{u}(t) + \boldsymbol{1}_n\lambda^*(t) + G^{\mathrm{T}}\boldsymbol{\epsilon}^*(t) = \boldsymbol{0} & \text{(5a)} \\ \boldsymbol{1}_n^{\mathrm{T}}\boldsymbol{m}(t) - k = 0 & \text{(5b)} \\ F_\iota(\boldsymbol{\epsilon}^*(t), \boldsymbol{\zeta} - G\boldsymbol{m}^*(t)) = \boldsymbol{0}(5c). & \text{(5c)} \end{cases}$$

Therefore, a compact matrix form is presented as follows:

$$\underbrace{\begin{bmatrix} \gamma I_n & \boldsymbol{1}_n & G^{\mathrm{T}} \\ \boldsymbol{1}_n^{\mathrm{T}} & 0 & \boldsymbol{0}_{2n}^{\mathrm{T}} \\ -G & \boldsymbol{0}_{2n} & I_{2n} \end{bmatrix}}_{\aleph\in\mathbb{R}^{(3n+1)\times(3n+1)}} \underbrace{\begin{bmatrix} \boldsymbol{m}^*(t) \\ \lambda^*(t) \\ \boldsymbol{\epsilon}^*(t) \end{bmatrix}}_{\boldsymbol{x}^*(t)\in\mathbb{R}^{3n+1}} - \underbrace{\begin{bmatrix} \boldsymbol{u}(t) \\ k \\ \boldsymbol{\psi}^*(t) - \boldsymbol{\zeta} \end{bmatrix}}_{\boldsymbol{y}^*(t)\in\mathbb{R}^{3n+1}} = \boldsymbol{0}, \tag{6}$$

where $I_{2n} \in \mathbb{R}^{2n\times 2n}$ is a $2n$-dimensional identity matrix, and the auxiliary vector $\boldsymbol{\psi}^*(t) \in \mathbb{R}^{2n}$ is defined as $\boldsymbol{\psi}^*(t) = \sqrt{\boldsymbol{\epsilon}^*(t)\circ\boldsymbol{\epsilon}^*(t) + \boldsymbol{\varpi}^*(t)\circ\boldsymbol{\varpi}^*(t) + \iota}$ with $\boldsymbol{\varpi}^*(t) = \boldsymbol{\zeta} - G\boldsymbol{m}^*(t)$. Note that the matrix $\aleph$ is nonsingular, and the vector $\boldsymbol{y}^*(t)$, which contains the output vector $\boldsymbol{m}^*(t)$, is expressed as a function of both the system state and time, that is, $\boldsymbol{y}^*(\boldsymbol{x}^*(t), t)$. The validity of the equation (4) holds under the assumption that the optimal solution $\boldsymbol{x}^*(t)$ is attained. Therefore, an error function is introduced as:

$$\boldsymbol{\chi}(t) = \aleph\boldsymbol{x}(t) - \boldsymbol{y}(\boldsymbol{x}(t), t). \tag{7}$$

2.2 | Network Design

To guarantee that the optimal solution is attainable, the error function $\boldsymbol{\chi}(t)$ needs to recursively converge to zero. Motivated by the dynamic formulation $\dot{\boldsymbol{\chi}}(t) = -\rho\boldsymbol{\chi}(t) - \sigma\int_0^t \boldsymbol{\chi}(\tau)\mathrm{d}\tau$, where $\rho, \sigma \in \mathbb{R}^+$ are scaling factors, a robust neurodynamic network is designed as:

$$\begin{aligned} \dot{\boldsymbol{x}}(t) = \mathcal{N}^{-1}(t)\Big(&\dot{\boldsymbol{y}}(\boldsymbol{x}(t), t) - \rho(\aleph\boldsymbol{x}(t) - \boldsymbol{y}(\boldsymbol{x}(t), t)) \\ &- \sigma\int_0^t (\aleph\boldsymbol{x}(\tau) - \boldsymbol{y}(\boldsymbol{x}(\tau), \tau))\mathrm{d}\tau + \boldsymbol{\mu}(t)\Big), \end{aligned} \tag{8}$$

where the matrix $\mathcal{N}(t) = [\gamma I_n, \mathbf{1}_n, G^{\mathrm{T}}; \mathbf{1}_n^{\mathrm{T}}, 0, \mathbf{0}_{2n}^{\mathrm{T}}; (\mathcal{N}_1(t) - I_{2n})G, \mathbf{0}_{2n}, I_{2n} - \mathcal{N}_2(t)]$ with $\mathcal{N}_1(t) = \mathrm{diag}(\varpi(t) \oslash \psi(t))$, $\mathcal{N}_2(t) = \mathrm{diag}(\epsilon(t) \oslash \psi(t))$ and $\oslash$ denoting the Hadamard division; superscript $(\cdot)^{-1}$ denotes the matrix inversion; and $\mu(t)$ is the noise vector. Owing to its asymptotic convergence and inherent robustness against noise, this network guarantees that the system state converges to the desired equilibrium point. Furthermore, in view of the prevalent slow convergence issue in multi-agent systems, a nonlinear activation function is introduced to expedite the convergence process and is defined as follows:

$$\mathcal{H}(\theta_i) = \begin{cases} a_1|\theta_i|^{\wp} + a_2\theta_i, & \theta_i > 0 \\ 0, & \theta_i = 0 \\ -a_1|\theta_i|^{\wp} + a_2\theta_i, & \theta_i < 0, \end{cases} \tag{9}$$

with $\wp \in [0, 1]$ and $a_1, a_2 \in \mathbb{R}^+$ being positive design parameters that control the slope and saturation characteristics of the function. Therefore, the ACNT-kWTA network is constructed as follows:

$$\begin{aligned} \dot{\boldsymbol{x}}(t) = \mathcal{N}^{-1}(t)\Big(&\dot{\boldsymbol{y}}(\boldsymbol{x}(t), t) - \rho\mathcal{H}(\aleph\boldsymbol{x}(t) - \boldsymbol{y}(\boldsymbol{x}(t), t)) \\ &- \sigma\int_0^t (\aleph\boldsymbol{x}(\tau) - \boldsymbol{y}(\boldsymbol{x}(\tau), \tau))\mathrm{d}\tau + \mu(t)\Big). \end{aligned} \tag{10}$$

2.3 | Model Construction

In multi-agent systems, a given task can be accomplished efficiently by selected winners, identified through the ACNT-kWTA network (10). However, equality constraint (2b) involves summing over all outputs (i.e., $\mathbf{1}_n^{\mathrm{T}}\boldsymbol{m}(t) = k$), which represents a centralised approach. To enable distributed operation, consensus-based estimators are leveraged, allowing agents to collectively determine the winners using only local interactions. Thereinto, the graph-theoretic concepts in multi-agent systems are introduced, focussing on relationships between agents, such as nodes, edges and connectivity. For a system with n agents, the communication topology is modelled by a graph $\mathcal{G} = (\mathcal{V}, \mathcal{E}, \mathcal{A})$ where $\mathcal{V} = \{1, 2, ..., n\}$ is the node set, $\mathcal{E} \subseteq \mathcal{V} \times \mathcal{V}$ is the edge set and $\mathcal{A} = [a_{ij}] \in \mathbb{R}^{n\times n}$ is the adjacency matrix. To govern the interaction topology among agents, the communication links are established based on the relative Euclidean distances among agents. Specifically, the adjacency element $a_{ij} \in \{0, 1\}$ is defined as:

$$a_{ij} = \begin{cases} 1, & \text{if distance}(i, j) < d \\ 0, & \text{if distance}(i, j) \geq d, \end{cases} \tag{11}$$

where $d \in \mathbb{R}^+$ is the maximum communication range. It is assumed that the resulting graph $\mathcal{G}$ remains connected throughout the entire operation, which is a necessary condition for the distributed kWTA model to propagate information across the whole network. Additionally, existing consensus-based kWTA models typically assume that the communication between agents is free from disturbances [24–26]. In practice, multi-agent systems often face challenges in achieving consensus estimation due to factors such as communication disturbances, computational errors, sensor noise and environmental fluctuations.

Moreover, the coexistence of communication disturbances and noise will severely compromise the consensus performance and competitive decision-making of distributed multi-agent systems. Inspired by the concept of disturbance observers in control theory, a robust consensus estimator that incorporates a real-time noise observer to estimate and compensate for unknown stochastic disturbances is introduced as:

$$\begin{aligned} \dot{\boldsymbol{s}}_i(t) &= \boldsymbol{z}_i(t) + \eta_i(t) \\ \dot{\boldsymbol{z}}_i(t) &= \kappa(\boldsymbol{m}_i(t) - \boldsymbol{s}_i(t)) + \kappa_1\sum_{j\in N_i} a_{ij}(\boldsymbol{s}_j(t) - \boldsymbol{s}_i(t)) \\ &\quad + \kappa_2\boldsymbol{v}_i(t) - \hat{\eta}_i(t) \\ \dot{\boldsymbol{v}}_i(t) &= \sum_{j\in N_i} a_{ij}(\boldsymbol{s}_j(t) - \boldsymbol{s}_i(t)) \\ \dot{\boldsymbol{\phi}}_i(t) &= -\nu\boldsymbol{\phi}_i(t) - \nu^2\boldsymbol{s}_i(t) - \nu\boldsymbol{z}_i(t) \\ \hat{\eta}_i(t) &= \boldsymbol{\phi}_i(t) + \nu\boldsymbol{s}_i(t), \end{aligned} \tag{12}$$

where $\boldsymbol{s}(t)$ is the agent's average estimator for $k/\sum_i^n \boldsymbol{m}_i(t)$; $\boldsymbol{z}(t)$, $\boldsymbol{v}(t)$ and $\boldsymbol{\phi}(t)$ are states variables; $\eta(t)$ denotes the communication disturbances; $\hat{\eta}(t)$ is the estimator of $\eta(t)$; κ, κ_1, κ_2 and $\nu \in \mathbb{R}^+$ are convergence factors.

Based on the proposed ACNT-kWTA network (10) and the developed robust consensus estimator (12), an ERCC model is constructed, which exhibits strong resilience against noise and communication disturbances. Due to leveraging consensus for state estimation under limited communication in the model, the ERCC model is presented as:

$$\begin{aligned} \dot{\boldsymbol{x}}(t) = \mathcal{N}^{-1}(t)\Big(&\dot{\hat{\boldsymbol{y}}}(\boldsymbol{x}(t), t) - \rho\mathcal{H}\Big(\hat{\aleph}\boldsymbol{x}(t) - \hat{\boldsymbol{y}}(\boldsymbol{x}(t), t)\Big) \\ &- \sigma\int_0^t \Big(\hat{\aleph}\boldsymbol{x}(\tau) - \hat{\boldsymbol{y}}(\boldsymbol{x}(\tau), \tau)\Big)\mathrm{d}\tau + \mu(t)\Big), \end{aligned} \tag{13}$$

where vector $\hat{\boldsymbol{y}}(\boldsymbol{x}(t), t) = [\boldsymbol{u}(t); \sum_{i=0}^n \boldsymbol{s}_i(t) = k; \psi(t) - \zeta]$; matrix $\hat{\aleph} = [\mu I_n, \mathbf{1}_n, G^{\mathrm{T}}; \mathbf{0}_n^{\mathrm{T}}, 0, \mathbf{0}_{2n}^{\mathrm{T}}; -G, \mathbf{0}_{2n}, I_{2n}]$; and vector $\boldsymbol{s}(t) = \boldsymbol{x}(t)[1 : n]$.

2.4 | Existing Models

To demonstrate the advantages of the proposed model, three existing kWTA comparative models are presented. First, a distributed-allowed noise-resistant kWTA (DANR-kWTA) network incorporating a consensus estimator is presented in [36]. Its expression is given as follows:

$$\begin{aligned} \dot{\boldsymbol{x}}(t) = \mathcal{N}^{-1}(t)\Big(&\dot{\hat{\boldsymbol{y}}}(\boldsymbol{x}(t), t) - \rho_1\mathcal{H}_1\Big(\hat{\aleph}\boldsymbol{x}(t) - \hat{\boldsymbol{y}}(\boldsymbol{x}(t), t)\Big) \\ &- \rho_2\mathcal{H}_2\Big(\hat{\aleph}\boldsymbol{x}(t) - \hat{\boldsymbol{y}}(\boldsymbol{x}(t), t) \\ &+ \rho_1\int_0^t \mathcal{H}_1\Big(\hat{\aleph}\boldsymbol{x}(\tau) - \hat{\boldsymbol{y}}(\boldsymbol{x}(\tau), \tau)\Big)\mathrm{d}\tau + \mu(t)\Big)\Big) \\ \dot{\boldsymbol{s}}_i(t) = -\kappa_3\Big(&\sum_{j\in N_i} a_{ij}(\boldsymbol{s}_i(t) - \boldsymbol{s}_j(t)) + (\boldsymbol{m}_i(t) - \boldsymbol{s}_i(t)) \\ &+ \sum_{j\in N_i} a_{ij}(\boldsymbol{v}_i(t) - \boldsymbol{v}_j(t))\Big) \\ \dot{\boldsymbol{v}}_i(t) = &\sum_{j\in N_i} a_{ij}(\boldsymbol{s}_i(t) - \boldsymbol{s}_j(t)), \end{aligned} \tag{14}$$

where ρ_1, ρ_2, and $\kappa_3 \in \mathbb{R}^+$ are convergence factors; $\mathcal{H}_1(\cdot)$ is a linear activation function; and $\mathcal{H}_2(\boldsymbol{c})$ is a bounded activation function defined element-wise as $\mathcal{H}_2(\boldsymbol{c}_i) = \boldsymbol{c}_i$ for $|\boldsymbol{c}_i| < 1$, $\mathcal{H}_2(\boldsymbol{c}_i) = 1$ for $\boldsymbol{c}_i > 1$, and $\mathcal{H}_2(\boldsymbol{c}_i) = -1$ for $\boldsymbol{c}_i < -1$.

Second, a communication-time-delay-considering kWTA (CTDC-kWTA) network, which also integrates a consensus estimator, is presented in [37]. Its mathematical formulation is given as:

$$\begin{aligned}
\dot{\boldsymbol{x}}(t) &= \mathcal{N}^{-1}(t)\Big(\dot{\widehat{\boldsymbol{y}}}(\boldsymbol{x}(t), t) - \rho_3 \mathcal{H}_2\Big(\widehat{\aleph}\boldsymbol{x}(t) - \widehat{\boldsymbol{y}}(\boldsymbol{x}(t), t)\Big)\Big) \\
\dot{\boldsymbol{s}}_i(t) &= -\kappa_4\Bigg(\sum_{j\in N_i} a_{ij}\big(\boldsymbol{s}_i(t-\tau) - \boldsymbol{s}_j(t-\tau)\big) \\
&\quad + (\boldsymbol{m}_i(t) - \boldsymbol{s}_i(t)) + \sum_{j\in N_i} a_{ij}\big(\boldsymbol{v}_i(t) - \boldsymbol{v}_j(t)\big)\Bigg) \\
\dot{\boldsymbol{v}}_i(t) &= \sum_{j\in N_i} a_{ij}\big(\boldsymbol{s}_i(t-\tau) - \boldsymbol{s}_j(t-\tau)\big),
\end{aligned} \tag{15}$$

where $\rho_3, \kappa_4 \in \mathbb{R}^+$ are convergence factors.

Third, a distributed dynamic task allocation kWTA (DDTA-kWTA) network [38] is expressed as:

$$\begin{aligned}
\kappa_5 \dot{\boldsymbol{m}} &= -\boldsymbol{m} + \frac{\mathcal{H}_2(\boldsymbol{u} - \boldsymbol{\varpi})}{\varepsilon} \\
\kappa_5 \dot{\boldsymbol{\omega}} &= \frac{L\boldsymbol{\varpi}}{\varepsilon} \\
\kappa_5 \dot{\boldsymbol{\varpi}} &= \frac{n\boldsymbol{m} - k\mathbf{1} - nL\boldsymbol{\omega} - nL\boldsymbol{\varpi}}{n\varepsilon},
\end{aligned} \tag{16}$$

where $\kappa_5 \in \mathbb{R}^+$ denotes a convergence factor; $\varepsilon \in \mathbb{R}^+$ stands for a design parameter; L is a graph Laplacian matrix; and $\boldsymbol{\omega}, \boldsymbol{\varpi} \in \mathbb{R}^n$ are auxiliary vectors.

3 | Theoretical Analyses and Results

This section focuses on the theoretical analysis of the stability and convergence of the ACNT-kWTA network under both ideal and noisy environments. Furthermore, the robustness of the developed consensus estimator is evaluated in the presence of communication disturbances.

Theorem 1. *For the noise-free case, the error norm $\|\boldsymbol{\chi}(t)\|_2$ of the proposed ACNT-kWTA network (10) converges asymptotically to zero from any initial condition $\boldsymbol{\chi}(0)$ where $\|\cdot\|_2$ denotes the Euclidean 2-norm. Consequently, the first n elements of vector $\boldsymbol{x}(t)$ converge to the optimal solution $\boldsymbol{m}(t)$ of kWTA problem (1).*

Proof: In the noise-free scenario, the proposed ACNT-kWTA network (10) is rewritten as:

$$\dot{\boldsymbol{\chi}}(t) = -\rho\mathcal{H}(\boldsymbol{\chi}(t)) - \sigma\int_0^t \boldsymbol{\chi}(\tau)\mathrm{d}\tau. \tag{17}$$

To facilitate the convergence analysis of $\boldsymbol{\chi}(t)$, an auxiliary vector is introduced as $\boldsymbol{\omega}(t) = \int_0^t \boldsymbol{\chi}(\tau)\,\mathrm{d}\tau$. It follows that:

$$\dot{\boldsymbol{\omega}}(t) = \boldsymbol{\chi}(t). \tag{18}$$

Therefore, (17) is reformulated as:

$$\dot{\boldsymbol{\chi}}(t) = -\rho\,\mathcal{H}(\boldsymbol{\chi}(t)) - \sigma\,\boldsymbol{\omega}(t). \tag{19}$$

Given the Lyapunov function candidate as follow:

$$\mathcal{L}_1(t) = \frac{1}{2}\boldsymbol{\chi}^{\mathrm{T}}(t)\boldsymbol{\chi}(t) + \frac{\sigma}{2}\boldsymbol{\omega}^{\mathrm{T}}(t)\boldsymbol{\omega}(t). \tag{20}$$

Since $\sigma > 0$, $\mathcal{L}_1(t)$ is positive definite and radially unbounded. Taking the time derivative of (20) yields:

$$\begin{aligned}
\dot{\mathcal{L}}_1(t) &= \boldsymbol{\chi}^{\mathrm{T}}(t)(-\rho\,\mathcal{H}(\boldsymbol{\chi}(t)) - \sigma\,\boldsymbol{\omega}(t)) + \sigma\,\boldsymbol{\omega}^{\mathrm{T}}(t)\dot{\boldsymbol{\omega}}(t) \\
&= -\rho\boldsymbol{\chi}^{\mathrm{T}}(t)\mathcal{H}(\boldsymbol{\chi}(t)).
\end{aligned} \tag{21}$$

Given that $\mathcal{H}(\cdot)$ is odd and monotonically increasing, it satisfies $\boldsymbol{\chi}_i(t)\,\mathcal{H}(\boldsymbol{\chi}_i(t)) \geq 0$ where the equality holds if and only if $\boldsymbol{\chi}_i(t) = 0$. In addition, for $0 < \wp < 1$, the map $\theta_i \to |\theta_i|^{\wp}$ is globally Hölder continuous, whereas the linear term $a_2\theta_i$ is Lipschitz continuous. Hence, $\mathcal{H}(\cdot)$ is globally uniformly continuous. From $\dot{\mathcal{L}}_1(t) \leq 0$, it follows that $\mathcal{L}_1(t)$ is nonincreasing and bounded below, which implies $\int_0^{\infty}(-\dot{\mathcal{L}}_1(\tau))\mathrm{d}\tau = \mathcal{L}_1(0) - \lim_{t\to\infty}\mathcal{L}_1(t) < \infty$. Moreover, $\boldsymbol{\chi}(t)$ and $\boldsymbol{\omega}(t)$ are bounded, and $\mathcal{H}(\cdot)$ is Lipschitz continuous on bounded sets; thus $\dot{\boldsymbol{\chi}}(t)$ is bounded. It follows that $\boldsymbol{\chi}^{\mathrm{T}}(t)\mathcal{H}(\boldsymbol{\chi}(t))$ has a bounded time derivative, so $\dot{\mathcal{L}}_1(t)$ is uniformly continuous. By Barbalat's lemma [39], we conclude $\dot{\mathcal{L}}_1(t) \to 0$, as $t \to \infty$. From the preceding analysis, we have $\boldsymbol{\chi}^{\mathrm{T}}(t)\,\mathcal{H}(\boldsymbol{\chi}(t)) = \sum_{i=1}^{3n+1} \boldsymbol{\chi}_i(t)\,\mathcal{H}(\boldsymbol{\chi}_i(t)) \to 0$ as $t \to \infty$. Since $\mathcal{H}(\cdot)$ is odd and strictly increasing, it follows that $\boldsymbol{\chi}_i(t) \to 0$ as $t \to \infty$ for each i. This implies that the error norm $\|\boldsymbol{\chi}(t)\|_2$ of the ACNT-kWTA network converges to zero globally and asymptotically. As a result, the first n elements of vector $\boldsymbol{x}(t)$ converge to the optimal solution $\boldsymbol{m}(t)$ of kWTA problem (1). The proof is completed. ■

Theorem 2. *Consider the proposed ACNT-kWTA network (10) to solve kWTA problem (1) under a linear time-varying noise $\boldsymbol{\mu}(t) = \bar{\boldsymbol{\mu}}\,t + \tilde{\boldsymbol{\mu}}$, where $\bar{\boldsymbol{\mu}}$ and $\tilde{\boldsymbol{\mu}}$ are constant vectors. Assume that the network parameter satisfies $c = 2\rho a_2 - 1 > 0$. Then the error norm satisfies $\lim_{t\to\infty} sup\|\boldsymbol{\chi}(t)\|_2 \leq \|\bar{\boldsymbol{\mu}}\|_2/\sqrt{\sigma c}$ (i.e., $\|\boldsymbol{\chi}(t)\|_2$ converges to a bounded region of radius $\|\bar{\boldsymbol{\mu}}\|_2/\sqrt{\sigma c}$). Moreover, as $\sigma \to +\infty$, the steady-state error satisfies $\lim_{t\to\infty}\|\boldsymbol{\chi}(t)\|_2 = 0$.*

Proof: When subjected to a linear time-varying noise, (10) is rewritten as:

$$\dot{\boldsymbol{\chi}}(t) = -\rho\mathcal{H}(\boldsymbol{\chi}(t)) - \sigma\int_0^t \boldsymbol{\chi}(\tau)\mathrm{d}\tau + \boldsymbol{\mu}(t). \tag{22}$$

Recalling the auxiliary vector (18), one has:

$$\dot{\boldsymbol{\chi}}(t) = -\rho\mathcal{H}(\boldsymbol{\chi}(t)) - \sigma\boldsymbol{\omega}(t) + \boldsymbol{\mu}(t). \tag{23}$$

Letting $\overline{\boldsymbol{\omega}}(t) = \boldsymbol{\omega}(t) - \boldsymbol{\mu}(t)/\sigma$, it follows that $\dot{\overline{\boldsymbol{\omega}}}(t) = \boldsymbol{\chi}(t) - \bar{\boldsymbol{\mu}}/\sigma$. Define a Lyapunov candidate function as:

$$\mathcal{L}_2(t) = \frac{1}{2}\,\boldsymbol{\chi}^{\mathrm{T}}(t)\boldsymbol{\chi}(t) + \frac{\sigma}{2}\overline{\boldsymbol{\omega}}^{\mathrm{T}}(t)\overline{\boldsymbol{\omega}}(t). \tag{24}$$

Differentiating (24) with respect to time gives:

$$\begin{aligned}\dot{\mathcal{L}}_2(t) &= \chi^{\mathrm{T}}(t)(-\rho\,\mathcal{H}(\chi(t)) - \sigma\overline{\omega}(t)) + \sigma\overline{\omega}^{\mathrm{T}}(t)\left(\chi(t) - \frac{\overline{\mu}}{\sigma}\right) \\ &= -\rho\chi^{\mathrm{T}}(t)\mathcal{H}(\chi(t)) - \overline{\omega}^{\mathrm{T}}(t)\overline{\mu}.\end{aligned} \tag{25}$$

Considering the nonlinear activation function $\mathcal{H}(\chi_i)\ (t) = a_1|\chi_i(t)|^{\wp}\mathrm{sign}\left(\chi_i(t)\right) + a_2\chi_i(t)$ $(0 < \wp < 1,\ a_1, a_2 > 0)$, one has:

$$-\rho\chi^{\mathrm{T}}(t)\mathcal{H}(\chi(t)) \le -\rho a_2\|\chi(t)\|_2^2. \tag{26}$$

Using Young's inequality, one obtains:

$$-\overline{\omega}^{\mathrm{T}}(t)\overline{\mu} \le \frac{\sigma}{2}\|\overline{\omega}(t)\|_2^2 + \frac{\|\overline{\mu}\|_2^2}{2\sigma}. \tag{27}$$

Therefore, (25) is reformulated as:

$$\dot{\mathcal{L}}_2(t) \le -\rho a_2\|\chi(t)\|_2^2 + \frac{\sigma}{2}\|\overline{\omega}(t)\|_2^2 + \frac{\|\overline{\mu}\|_2^2}{2\sigma}. \tag{28}$$

Leveraging the inequality equations $\mathcal{L}_2(t) \ge 1/2\|\chi(t)\|_2^2$ and $\mathcal{L}_2(t) \ge \sigma/2\|\overline{\omega}(t)\|_2^2$, there exists a positive constant $c = 2\rho a_2 - 1$, and we have:

$$\dot{\mathcal{L}}_2(t) \le -c\mathcal{L}_{(t)} + \frac{\|\overline{\mu}\|_2^2}{2\sigma}. \tag{29}$$

Therefore, the following bound holds:

$$\mathcal{L}_2(t) \le e^{-ct}\mathcal{L}_2(0) + \frac{\|\overline{\mu}\|_2^2}{2\sigma c}. \tag{30}$$

Note that the exponential term $e^{-ct}\mathcal{L}_2(0)$ decays to zero as $t \to \infty$. Thus, we obtain:

$$\limsup_{t\to\infty}\mathcal{L}_2(t) \le \frac{\|\overline{\mu}\|_2^2}{2\sigma c}. \tag{31}$$

Since $\|\chi(t)\|_2^2 \le 2\,\mathcal{L}_2(t)$, taking the upper limit and square root on both sides yields:

$$\limsup_{t\to\infty}\|\chi(t)\|_2 \le \sqrt{2\limsup_{t\to\infty}\mathcal{L}_2(t)} \le \sqrt{2\frac{\|\overline{\mu}\|_2^2}{2\sigma c}} = \frac{\|\overline{\mu}\|_2}{\sqrt{\sigma c}}. \tag{32}$$

Hence, even under linear time-varying noise, the error norm $\|\chi(t)\|_2$ of ACNT-kWTA network (10) solving kWTA problem (1) converges to a bounded region given by $\|\overline{\mu}\|_2/\sqrt{\sigma c}$. Additionally, it is obvious that as $\sigma \to +\infty$, the steady-state error $\lim_{t\to\infty}\|\chi(t)\|_2$ tends to zero. Hence, the first n elements of vector $\boldsymbol{x}(t)$ converge to the optimal solution $\boldsymbol{m}(t)$ of kWTA problem (1). The proof is completed. ■

Theorem 3. *Under a bounded random noise satisfying* $\|\mu(t)\|_2 \le \Delta$ *almost surely for all* $t \ge 0$ *where* $\Delta > 0$ *is a constant, the error norm* $\|\chi(t)\|_2$ *of the ACNT-kWTA network (10) for solving the kWTA problem (1) is globally ultimately bounded. Specifically, an explicit transient bound is established as* $\|\chi(t)\|_2 \le \exp(-(\rho a_2/2)t)\|\chi(0)\|_2 + \Delta/\rho a_2(1-\exp(-(\rho a_2/2)t))$. *Moreover,* $\lim_{t\to\infty}sup\|\chi(t)\|_2 \le \Delta/(\rho a_2)$, *which indicates that the tracking error exponentially converges to a bounded neighbourhood of the origin, and the steady-state bound decreases inversely with* ρ.

Proof: When subjected to a bounded random noise, (10) is rewritten as:

$$\dot{\chi}(t) = -\rho\mathcal{H}(\chi(t)) - \sigma\omega(t) + \mu(t), \tag{33}$$

with $\dot{\omega}(t) = \chi(t)$. Define a Lyapunov candidate function as:

$$\mathcal{L}_3(t) = \frac{1}{2}\chi^{\mathrm{T}}(t)\chi(t) + \frac{\sigma}{2}\omega^{\mathrm{T}}(t)\omega(t), \tag{34}$$

which is positive definite and radially unbounded. The time derivative of $\mathcal{L}_3(t)$ is computed as:

$$\begin{aligned}\dot{\mathcal{L}}_3(t) &= \chi^{\mathrm{T}}(t)(-\rho\,\mathcal{H}(\chi(t)) - \sigma\,\omega(t) + \mu(t)) + \sigma\,\omega^{\mathrm{T}}(t)\chi(t) \\ &= -\rho\,\chi^{\mathrm{T}}(t)\mathcal{H}(\chi(t)) + \chi^{\mathrm{T}}(t)\mu(t) \\ &\le -\rho a_2\|\chi(t)\|_2^2 + \chi^{\mathrm{T}}(t)\mu(t).\end{aligned} \tag{35}$$

Using Young's inequality, we obtain:

$$\begin{aligned}\chi^{\mathrm{T}}(t)\mu(t) &\le \frac{\rho a_2}{2}\|\chi(t)\|_2^2 + \frac{\|\mu(t)\|_2^2}{2\rho a_2} \\ &\le \frac{\rho a_2}{2}\|\chi(t)\|_2^2 + \frac{\Delta^2}{2\rho a_2}.\end{aligned} \tag{36}$$

Combining (35) and (36), and using the fact that $\mathcal{L}_3(t) \ge \|\chi(t)\|_2^2/2$, one has:

$$\begin{aligned}\dot{\mathcal{L}}_3(t) &\le -\frac{\rho a_2}{2}\|\chi(t)\|_2^2 + \frac{\Delta^2}{2\rho a_2} \\ &\le -\rho a_2\,\mathcal{L}_3(t) + \frac{\Delta^2}{2\rho a_2}.\end{aligned} \tag{37}$$

Accordingly, the following inequality holds:

$$\mathcal{L}_3(t) \le e^{-\rho a_2 t}\,\mathcal{L}_3(0) + \frac{\Delta^2}{2(\rho a_2)^2}\left(1 - e^{-\rho a_2 t}\right). \tag{38}$$

Since $\|\chi(t)\|_2^2 \le 2\,\mathcal{L}_3(t)$, from (38) we obtain:

$$\|\chi(t)\|_2 \le e^{-\frac{\rho a_2}{2}t}\|\chi(0)\|_2 + \frac{\Delta}{\rho a_2}\left(1 - e^{-\frac{\rho a_2}{2}t}\right). \tag{39}$$

Taking $\limsup_{t\to\infty}$ on both sides yields:

$$\limsup_{t\to\infty}\|\chi(t)\|_2 = \frac{\Delta}{\rho a_2}. \tag{40}$$

Hence, even under bounded random noise conditions, the proposed ACNT-kWTA network remains robust. The error norm $\|\chi(t)\|_2$ of the network (10) in solving kWTA problem (1) is

ultimately bounded. As $\sigma \to +\infty$, the error norm $\|\chi(t)\|_2$ tends to $\Delta/(\rho a_2)$. Moreover, the bound (40) scales linearly with the noise radius Δ and is inversely proportional to the damping gain ρa_2. The proof is completed. ■

Theorem 4. *Suppose that the communication disturbances $\eta_i(t)$ for each agent $i \in \mathcal{V}$ is bounded and its rate is bounded, that is, $\dot{\eta}_i \in L_\infty$ with $M = \|\dot{\eta}_i\|_\infty < \infty$. Then, the robust consensus estimator (12) guarantees that the estimation error $\boldsymbol{p}_i(t) = \widehat{\eta}_i(t) - \eta_i(t)$ is globally exponentially bounded by the following explicit transient bound, which holds for all $t \geq 0$, $\|\boldsymbol{p}_i(t)\| \leq \sqrt{2\exp(-\nu t)\|\boldsymbol{p}(0)\|_2 + M^2/2\nu^2(1-\exp(-\nu t))}$ with ultimate bound M_i/ν. Furthermore, steady-state norm of the estimation error, $\lim_{t\to\infty}\|\boldsymbol{p}(t)\|_2$, decreases to zero as v tends to positive infinity.*

Proof: According to the definition of $\boldsymbol{p}_i(t)$, its derivative is presented as follows:

$$\dot{\boldsymbol{p}}_i(t) = \dot{\widehat{\eta}}_i(t) - \dot{\eta}_i(t). \tag{41}$$

Substituting $\widehat{\eta}_i(t) = \boldsymbol{\phi}_i(t) + \nu \boldsymbol{s}_i(t)$, $\dot{\boldsymbol{\phi}}_i(t) = -\nu\boldsymbol{\phi}_i(t) - \nu^2\boldsymbol{s}_i(t) - \nu\boldsymbol{z}_i(t)$ and $\dot{\boldsymbol{s}}_i(t) = \boldsymbol{z}_i(t) + \eta_i(t)$ into (41) yields:

$$\begin{aligned}\dot{\boldsymbol{p}}_i(t) &= \left(\dot{\boldsymbol{\phi}}_i(t) + \nu\dot{\boldsymbol{s}}_i(t)\right) - \dot{\eta}_i(t)\\ &= \left(-\nu\boldsymbol{\phi}_i(t) - \nu^2\boldsymbol{s}_i(t) + \nu\eta_i(t)\right) - \dot{\eta}_i(t)\\ &= -\nu\left(\boldsymbol{\phi}_i(t) + \nu\boldsymbol{s}_i(t) - \eta_i(t)\right) - \dot{\eta}_i(t)\\ &= -\nu\left(\widehat{\eta}_i(t) - \eta_i(t)\right) - \dot{\eta}_i(t)\\ &= -\nu\boldsymbol{p}_i(t) - \dot{\eta}_i(t).\end{aligned} \tag{42}$$

Define the following Lyapunov candidate function as:

$$\mathcal{L}_4(t) = \frac{1}{2}\|\boldsymbol{p}(t)\|_2^2. \tag{43}$$

Taking the time derivative of $\mathcal{L}_4(t)$ and leveraging the Young's inequality, one has:

$$\begin{aligned}\dot{\mathcal{L}}_4(t) &= \boldsymbol{p}^{\mathrm{T}}(t)\left(-\nu\boldsymbol{p}(t) - \dot{\eta}(t)\right)\\ &= -\nu\|\boldsymbol{p}(t)\|_2^2 - \boldsymbol{p}^{\mathrm{T}}(t)\dot{\eta}(t)\\ &\leq -\nu\|\boldsymbol{p}(t)\|_2^2 + \frac{\nu}{2}\|\boldsymbol{p}(t)\|_2^2 + \frac{1}{2\nu}\|\dot{\eta}\|_2^2\\ &= -\nu\mathcal{L}_4(t) + \frac{1}{2\nu}\|\dot{\eta}(t)\|_2^2.\end{aligned} \tag{44}$$

Since $\|\dot{\eta}(t)\|_2 \leq M$, there is:

$$\mathcal{L}_4(t) \leq e^{-\nu t}\mathcal{L}_4(0) + \frac{M^2}{2\nu^2}\left(1 - e^{-\nu t}\right). \tag{45}$$

Substituting (43) into (45), we obtain:

$$\begin{aligned}\|\boldsymbol{p}(t)\|_2 &\leq \sqrt{2e^{-\nu t}\mathcal{L}_4(0) + \frac{M^2}{2\nu^2}(1 - e^{-\nu t})}\\ &= \sqrt{2e^{-\nu t}\|\boldsymbol{p}(0)\|_2 + \frac{M^2}{2\nu^2}(1 - e^{-\nu t})}.\end{aligned} \tag{46}$$

Taking the upper limit yields:

$$\limsup_{t\to\infty}\|\boldsymbol{p}_i(t)\|_2 \leq \frac{M}{\nu}. \tag{47}$$

Therefore, the estimation error $\boldsymbol{p}_i(t) = \widehat{\eta}_i(t) - \eta_i(t)$ is globally exponentially bounded. In particular, for all $t \geq 0$, $\|\boldsymbol{p}_i(t)\| \leq \sqrt{2\exp(-\nu t)\|\boldsymbol{p}(0)\|_2 + M^2/2\nu^2(1-\exp(-\nu t))}$. Moreover, the ultimate bound satisfies $\lim_{t\to\infty}\boldsymbol{p}_i(t) = M_i/\nu$. The proof is completed. ■

4 | Illustrative Examples

This section presents two illustrative examples to validate the performance of the proposed ACNT-kWTA network (10) and ERCC model (13). Specifically, simulation results are reported to substantiate the efficacy and robustness of ACNT-kWTA network (10), whereas the practicality of ERCC model (13) is validated through multi-agent target tracking tasks.

4.1 | Numerical Simulations

For numerical implementation, parameters are chosen as follows. Specifically, the inputs of kWTA problem (1) are composed of four time-varying sinusoidal waves, defined as $\boldsymbol{u}_i(t) = 2\sin(2\pi(0.3t + 0.2(i+1))) + t$ for $i = 1, 2, 3, 4$. Other parameters of ACNT-kWTA network (10) are set to $k = 2$, $\gamma = 2 \times 10^{-5}$, $\rho = 20$ and $\sigma = 500$. The duration of the simulation is $T = 10$ s. For comparative fairness, the corresponding parameters of the CTDC-kWTA network and the DDTA-kWTA network are set identically to those of ACNT-kWTA network (10). Note that the above two networks only employ the kWTA network components of their corresponding models in (15) and (16). To verify the robustness of the proposed ACNT-kWTA network (10), this section first introduces the linear noise $\boldsymbol{\mu}_i(t) = qt + p$, followed by the bounded random noise $\boldsymbol{\mu}_i(t) \in [g, g+5]$, where $q = 9.87$, $p = 10.21$ and $g = 10.58$ are obtained randomly. Simulation results are presented in Figures 2 and 3.

Specifically, Figure 2a shows that the proposed ACNT-kWTA network (10) accurately identifies two winners in real time under continuously increasing linear noise. The output responses closely align with theoretical expectations, confirming effective noise suppression. By contrast, Figure 2b reveals that the CTDC-kWTA network fails to distinguish winners from losers with its output deviating markedly from theoretical expectations. Similarly, the DDTA-kWTA network completely fails to distinguish winners and losers under the same noise condition, indicating its insufficient robustness against linear time-varying noise, as shown in Figure 2c. These observations are corroborated by the error norm trajectories in Figure 2d. The error norm of ACNT-kWTA network (10) decays rapidly to zero, indicating asymptotic convergence. Conversely, the error norm of the CTDC-kWTA network continuously rises and diverges as the noise increases, while that of the DDTA-kWTA network remains consistently high.

Comparative simulation results under the bounded random noise are presented in Figure 3. Specifically, as shown in Figure 3a, the proposed ACNT-kWTA network (10) accurately identifies the

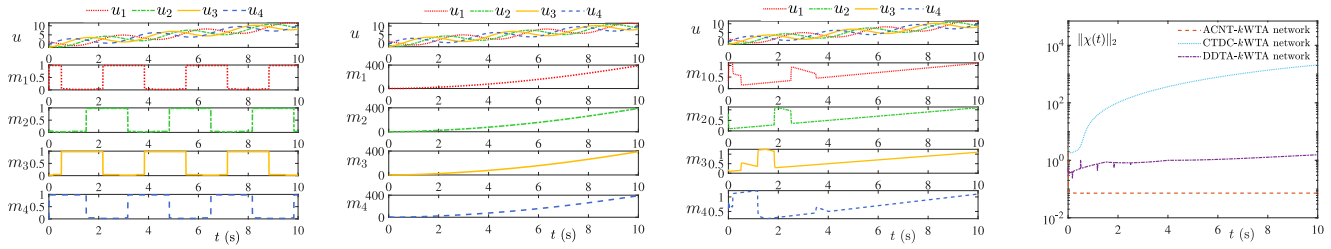


FIGURE 2 | Comparative simulation results of different networks for solving the time-varying kWTA problem under linear noise $\boldsymbol{\mu}_i(t) = qt + p$. (a) Input and output obtained by the proposed ACNT-kWTA network. (b) Input and output obtained by CTDC-kWTA network. (c) Input and output obtained by DDTA-kWTA network. (d) The error norm of different networks.

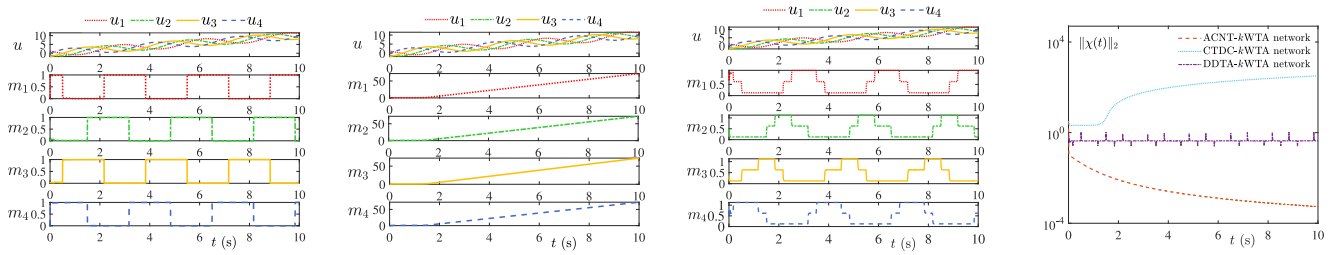


FIGURE 3 | Comparative simulation results of different networks for solving the time-varying kWTA problem under bounded random noise $\boldsymbol{\mu}_i(t) \in [g, g + 5]$. (a) Input and output obtained by the proposed ACNT-kWTA network. (b) Input and output obtained by CTDC-kWTA network. (c) Input and output obtained by DDTA-kWTA network. (d) The error norm of different networks.

two winners from the inputs. The smooth and stable output responses verify its effectiveness in suppressing random noise. In contrast, as shown in Figure 3b, the output of the CTDC-kWTA network continuously increases and fails to stabilise under random noise, a behaviour consistent with its performance under linear noise. Additionally, the DDTA-kWTA network is significantly affected by random noise, preventing stable winner and loser identification, as shown in Figure 3c. Moreover, the error norms of the three networks are shown in Figure 3d. The ACNT-kWTA network (10) rapidly converges to a bounded region around zero. Conversely, the error norm of the CTDC-kWTA network rapidly diverges over time, while that of the DDTA-kWTA network fluctuates and remains at a persistently high level. Overall, the proposed ACNT-kWTA network (10) achieves accurate and stable winner selection, demonstrating superior noise robustness over the existing networks.

4.2 | Multi-Agent Target Tracking Tasks

To verify the efficacy and robustness of the proposed ERCC model (13), this section reports simulation results alongside the physical experiment. To further assess its superiority, comparative simulations are carried out against the DANR-kWTA and CTDC-kWTA networks, each integrated with its own consensus estimator. For brevity, these two comparative models are referred to as DANR model (14) and CTDC model (15), respectively. Note that these models are evaluated under identical communication disturbances and noise to ensure fairness.

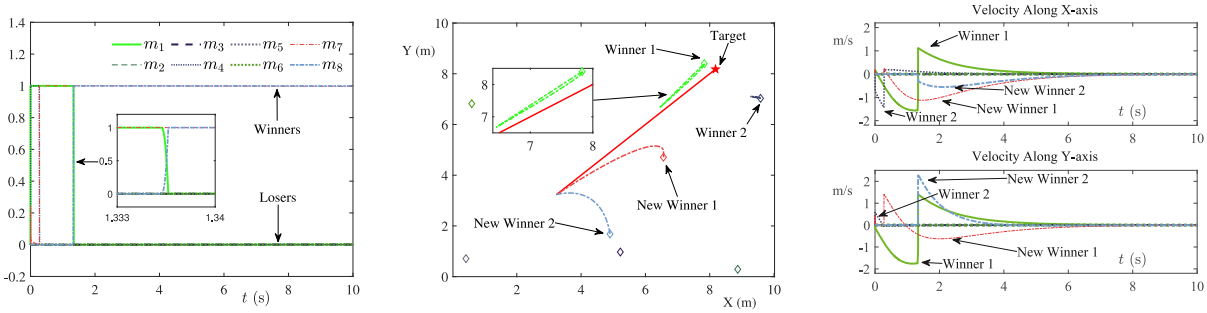
To verify the practicality of the proposed model, differential-driven wheeled mobile robots are employed in the simulation with each agent modelled as a single-integrator system [40]. Each agent is randomly placed within a square region of 10 m × 10 m at the start with its initial position denoted as $\boldsymbol{c}_i^0 \in \mathbb{R}^2$. Subsequently, the real-time positions of the ith agent and the target are represented by $\boldsymbol{c}_i(t) \in \mathbb{R}^2$ and $\boldsymbol{c}_0(t) \in \mathbb{R}^2$, respectively. The inputs to the ACNT-kWTA network are determined by the distance between the ith agent and the target, defined as $\boldsymbol{u}_i(t) = -\|\boldsymbol{c}_i(t) - \boldsymbol{c}_0(t)\|_2^2/2$. By utilising the proposed ACNT-kWTA network (13), the winner agents are selected to execute the tracking task. Thereafter, the control strategy for the ith agent is defined as:

$$\dot{\boldsymbol{c}}_i(t) = \varsigma\left(\boldsymbol{m}_i(t)\frac{\partial\left(\|\boldsymbol{c}_i(t) - \boldsymbol{c}_0(t)\|_2^2/2\right)}{\partial \boldsymbol{c}_i(t)} + (1 - \boldsymbol{m}_i(t))\frac{\partial\left(\|\boldsymbol{c}_i(t) - \boldsymbol{c}_i^0\|_2^2/2\right)}{\partial \boldsymbol{c}_i(t)}\right), \tag{48}$$

where $\varsigma \in \mathbb{R}^+$ is a velocity gain. This formulation ensures that winners track the target, whereas losers return to their initial positions. In addition, the relevant parameters are configured as follows: $n = 8$, $k = 2$, $\gamma = 2 \times 10^{-5}$, $\rho = 100$, $\sigma = 500$, $\kappa = 2000$, $\kappa_1 = 10$, $\kappa_2 = 10$, $\nu = 10$, $\varsigma = 7$, $\rho_1 = 100$, $\rho_2 = 100$, $\kappa_3 = 2000$, $\rho_3 = 100$, $\kappa_4 = 2000$, and the simulation duration is $T = 10$ s. Some of the above parameter settings are chosen to be as consistent as possible with those used in the previous numerical simulations, whereas the others are specifically tailored for the robust consensus estimator and comparison models, thereby helping ensure the reliability and reproducibility of the simulation results. To ensure fairness in

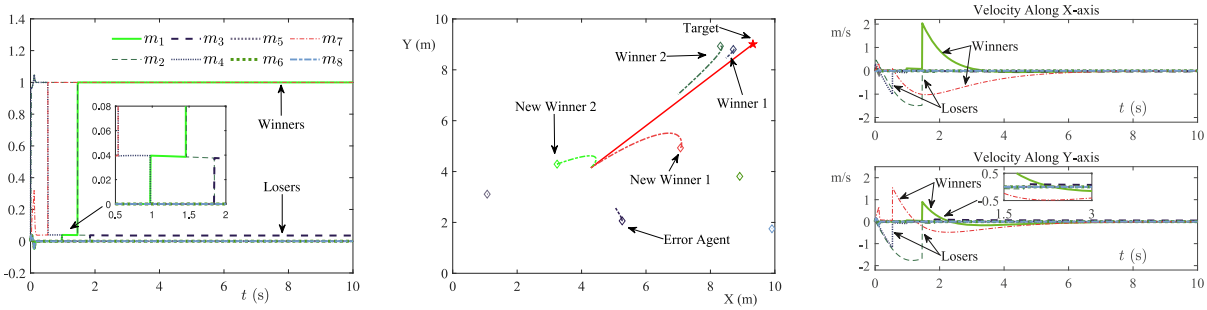
comparison, CTDC model (15) is simulated with a time delay set as $\tau = 0$ s. Furthermore, noise is introduced into the network, taking linear noise with a fixed bias $\boldsymbol{\mu}_i(t) = qt + p$ as an example, where $q = 3.13$ and $p = 9.58$ are obtained randomly, whereas the communication disturbance is modelled as $\boldsymbol{\eta}_i(t) = -3\sin(t)e^{-2t} + 3$. Moreover, the velocity of target is given as $\boldsymbol{z}(t) = -4e^{-t}\boldsymbol{c}_0(t)/\|\boldsymbol{c}_0(t)\|_2$ where $\boldsymbol{z}(t) \in \mathbb{R}^2$ denotes the horizontal position vector with components along the X- and Y-axes. Based on the above settings, simulation outcomes are shown in Figures 4–6, respectively.

The simulation results of the proposed ERCC model (13) are presented in Figure 4. As illustrated in Figure 4a, the kWTA outputs effectively differentiate winners from losers in real time, with 1 representing a winner and 0 representing a loser. Furthermore, the agents complete state updates within a very short period during winner transitions. The tracking trajectories of agents in pursuit of a moving target are shown in Figure 4b for intuitive visualisation. Throughout the process, two winners are always selected to pursue the target. In the initial stage, the agents labelled Winner 1 and Winner 2 are chosen based on their proximity to the target. Subsequently, two winner switches occur, and two new winners (i.e., labelled New Winner 1 and New Winner 2) are selected to track the moving target. Eventually, the new winners catch up with the target, indicating that the process has been successfully completed. The magnified inset illustrates that the loser executes a return action to its original position. The



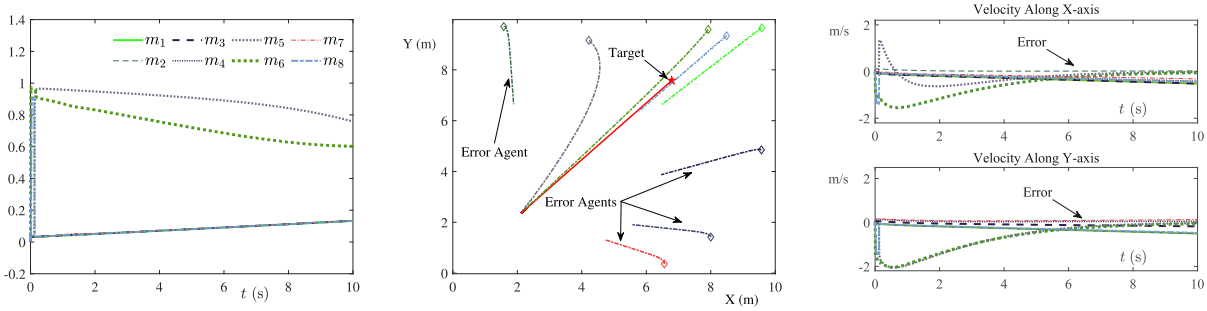
(a) (b) (c)

FIGURE 4 | Simulation results of the proposed ERCC model (13) in the multi-agent target tracking task. (a) Output of the kWTA network. (b) Trajectories of target and agents. (c) Velocities of each agent along the X- and Y-axes.



(a) (b) (c)

FIGURE 5 | Simulation results of DANR model (14) in multi-agent target tracking task. (a) Output of the kWTA network. (b) Trajectories of target and agents. (c) Velocities of each agent along the X- and Y-axes.



(a) (b) (c)

FIGURE 6 | Simulation results of CTDC model (15) in multi-agent target tracking task. (a) Output of the kWTA network. (b) Trajectories of target and agents. (c) Velocities of each agent along the X- and Y-axes.

entire tracking trajectory is smooth and continuous, showing the stability and robustness of the proposed model. Finally, Figure 4c depicts the velocity evolution of each agent in both X-axis and Y-axis directions; the axes are time (t in seconds) and speed (m/s), respectively. The velocities of winners gradually increase and decrease as they approach the target. During winner switching, the losers rapidly adjust their motion direction to return to their initial positions. Meanwhile, the velocities of the newly selected winners increase from zero and subsequently decrease as they move toward the target. These results highlight the strong dynamic decision-making capability and robustness of the proposed ERCC model (13).

To further validate the superiority of the proposed ERCC model (13), DANR model (14) and CTDC model (15) are implemented under identical simulation and disturbance conditions. The comparative results are shown in Figures 5 and 6. Specifically, Figures 5a and 6a demonstrate the kWTA outputs of the two comparison models. The results clearly indicate that DANR model (14) cannot achieve the same level of speed and accuracy in distinguishing winners from losers as the proposed ERCC model (13), whereas CTDC model (15) exhibits instability, failing to accurately complete the winner selection. The effect of this limitation on the tracking task is further demonstrated in the subsequent subfigures. For DANR model (14), as shown in Figure 5b, an erroneous agent is activated during the winner update process. The velocity of this agent along the Y-axis, depicted in Figure 5c, remains zero until approximately 2 s after which a nonzero velocity emerges. This behaviour indicates that the agent is mistakenly activated to participate in the tracking task. Similarly, in Figure 6b, CTDC model (15) exhibits instability during the tracking process due to the activation of multiple erroneous agents. As shown in Figure 6c, the velocity components of some agents along the X-axis and Y-axis continue to exist, further indicating that they are erroneously activated for the tracking task. In summary, both DANR model (14) and CTDC model (15) fail to achieve reliable kWTA performance under noise and communication disturbances, leading to reduced efficiency and erroneous agent activation. These results underscore the robustness and superiority of the proposed ERCC model (13).

Moreover, a multi-agent target tracking experiment is conducted on E-puck robots to further corroborate the efficacy and practicality of the proposed ERCC model (13) under the coexistence of noise and communication disturbances. The experimental setup involves six robots operating within a 0.9 m × 1.4 m workspace, employing a millimetre-scale high-frequency projection positioning system and a wireless communication control system. Each robot is equipped with a 32-bit STM32F4 microprocessor and a wireless receiver module [26]. In this setup, one robot serves as the moving target, whereas the other five function as tracking robots. The relevant parameters are consistent with those employed in prior simulations. The entire tracking process is described by six representative snapshots, as illustrated in Figure 7. At any given time, two optimal robots are chosen as the winners to track the target. Upon the emergence of new winners, the losers return directly to their initial positions. Notably, the dashed lines in the snapshots represent the return trajectories of the losers. Ultimately, two robots successfully track the target and accomplish the task.

To further highlight the contributions of the proposed ERCC model (13), a qualitative comparison with several representative studies is provided in Table 1. Although prior studies, such as [10, 24, 26, 36, 38], successfully adapt to time-varying inputs, apply to multi-agent systems and are mostly robust to noise, they fail to simultaneously handle the communication disturbances. In contrast, the proposed ERCC model (13) achieves accelerated convergence and noise resistance through the ACNT-kWTA network. Furthermore, unlike [10, 24, 26, 36], this paper develops a robust consensus estimator to simultaneously mitigate the impact of communication disturbances. Finally, the proposed ERCC model (13) is validated through numerical simulations and the physical experiment, demonstrating its superiority and effectiveness.

5 | Conclusions

This paper has proposed an ACNT-kWTA network incorporating a nonlinear activation function and an error-integral term, enabling it to rapidly and accurately obtain optimal solutions under noise conditions. In addition, a robust consensus estimator has been developed and integrated with the ACNT-kWTA network to construct an ERCC model, which is capable of simultaneously suppressing noise and communication disturbances. Theoretical analyses and numerical simulations have been provided to prove

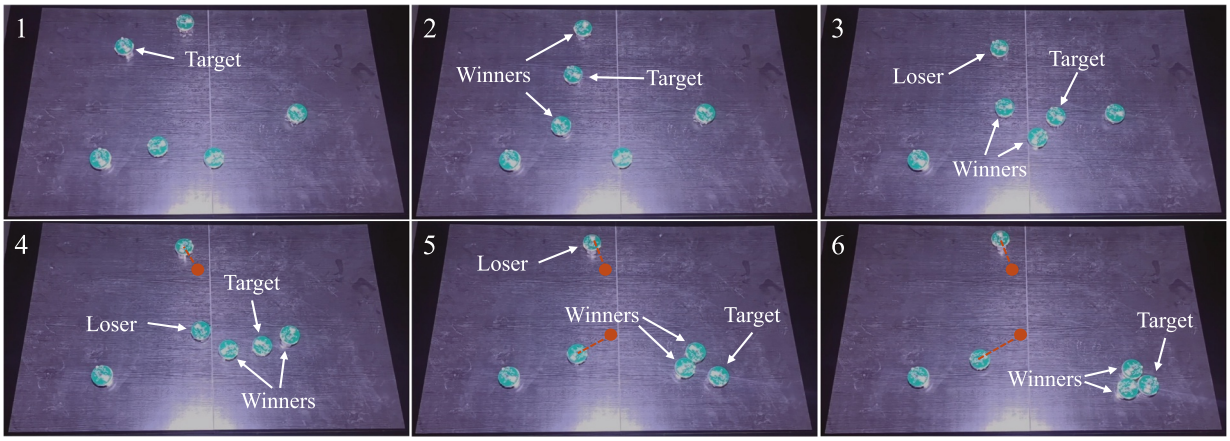


FIGURE 7 | Snapshots of a target tracking experiment based on the proposed ERCC model (13) on the E-puck2 platform.

TABLE 1 | Comparisons of existing *k*WTA models.

Related studies	Year	Time-varying inputs	Accelerated convergence	Noise robustness	Communication robustness	Multi-agent system applications	Physical experiment
This paper	2026	Yes	Yes	Yes	Yes	Yes	Yes
Paper [10]	2025	Yes	No	Yes	No	Yes	No
Paper [23]	2024	No	No	No[a]	No	No	No
Paper [24]	2026	Yes	No	Yes	No	Yes	No
Paper [26]	2025	Yes	No	Yes	No	Yes	Yes
Paper [36]	2025	Yes	Yes	Yes	No	Yes	No
Paper [38]	2025	Yes	No	No	No	Yes	No

[a]Noise is considered or analysed without an active suppression mechanism; therefore, it is not regarded as full noise robustness in this table.

the global convergence and robustness of the model. Moreover, the proposed model is deployed on E-puck robots for a multi-agent target tracking task to substantiate its efficacy and practicality. Future work will focus on developing a *k*WTA competitive coordination model that can resist false data injection attacks and incorporate collision avoidance, thereby enhancing the robustness and safety of multi-robot systems.

Acknowledgements

The authors would like to acknowledge the support of the Project of the National Natural Science Foundation of China (62666057); Leading Talent of the Qinghai Province Kunlun Talents Programme · High-Level Innovative and Entrepreneurial Talents (QHKLYC-GDCXCY-2024-359); the Project of EU Horizon INSTANT Grant 101236387; the Project of the Natural Science Foundation of the Qinghai (2026-ZJ-941M); the Project of the Key Laboratory of Tibetan Information Processing, Ministry of Education (QHSF-CS-2611, QHSF-CS-2607).

Conflicts of Interest

The authors declare no conflicts of interest.

Data Availability Statement

The data that support the findings of this study are available from the corresponding author upon reasonable request.

References

1. C. Diaz-Vilor, M. Barzegaran, and H. Jafarkhani, "Multi-UAV Energy-Efficient Wildfire Coverage Optimization," *IEEE Transactions on Wireless Communications* 24, no. 10 (October 2025): 8633–8648, https://doi.org/10.1109/twc.2025.3567953.

2. A. Nitti, M. D. de Tullio, I. Federico, and G. Carbone, "A Collective Intelligence Model for Swarm Robotics Applications," *Nature Communications* 16, no. 1 (July 2025): 6572, https://doi.org/10.1038/s41467-025-61985-7.

3. S. Basak, B. Dey, and B. Bhattacharyya, "Demand Side Management for Solving Environment Constrained Economic Dispatch of a Microgrid System Using Hybrid MGWOSCACSA Algorithm," *CAAI Transactions on Intelligence Technology* 7, no. 2 (June 2022): 256–267, https://doi.org/10.1049/cit2.12080.

4. D. Ma, J. Lv, C. Xu, and L. Jin, "Logic-Adaptive Discrete Neural Dynamics for Distributed Cooperative Control of Multi-Robot Systems via Minimum Infinity Norm Optimization," *IEEE Transactions on Fuzzy Systems* 34, no. 2 (February 2026): 531–539, https://doi.org/10.1109/tfuzz.2025.3642241.

5. Q. Ren, Y. Sun, S. Bian, and M. Magno, "Optimizing Energy Consumption and Coverage in Underwater Magnetic Induction-Assisted Acoustic WSNs Using Learning Automata-Based Cooperative MIMO Formation," *IEEE Transactions on Network Science and Engineering* 12, no. 5 (September–October 2025): 3527–3540, https://doi.org/10.1109/tnse.2025.3561751.

6. C. Hua, X. Cao, J. Li, and S. Li, "Fixed-Time Zeroing Neural Dynamics for Adaptive Coordination of Multi-Agent Systems," *CAAI Transactions on Intelligence Technology* 11, no. 1 (February 2026): 267–278, https://doi.org/10.1049/cit2.70089.

7. J. Lv, B.-G. Kim, K. Li, and H. Lu, "Multi-Agent Reinforcement Learning Driven Dynamic Resource Optimisation in Healthcare Transportation Networks," *CAAI Transactions on Intelligence Technology* 11, no. 2 (April 2026): 316–331, https://doi.org/10.1049/cit2.70125.

8. J. Wang, Y. Hong, J. Wang, et al., "Cooperative and Competitive Multi-Agent Systems: From Optimization to Games," *IEEE/CAA Journal of Automatica Sinica* 9, no. 5 (May 2022): 763–783, https://doi.org/10.1109/jas.2022.105506.

9. J. Ye, H. Gao, M. Hu, et al., "Learning-Based Tracking Control of AUV: Mixed Policy Improvement and Game-Based Disturbance Rejection," *CAAI Transactions on Intelligence Technology* 10, no. 2 (April 2025): 510–528, https://doi.org/10.1049/cit2.12372.

10. X. Cao, Y. Yang, S. Li, and V. N. Katsikis, "*k*-Winner-Take-All Competition Based on Novel Dynamic Neural Networks," *IEEE Transactions on Systems, Man, and Cybernetics: Systems* 55, no. 12 (December 2025): 9255–9265, https://doi.org/10.1109/tsmc.2025.3614997.

11. M. Eser and A. E. Yilmaz, "A Gossip-Based Auction Algorithm for Decentralized Task Rescheduling in Heterogeneous Drone Swarms," *IEEE Transactions on Aerospace and Electronic Systems* 61, no. 3 (June 2025): 6673–6696, https://doi.org/10.1109/taes.2025.3528390.

12. Y. Zhang, S. Li, and J. Weng, "Distributed *k*-Winners-Take-All Network: An Optimization Perspective," *IEEE Transactions on Cybernetics* 53, no. 8 (August 2023): 5069–5081, https://doi.org/10.1109/tcyb.2022.3170236.

13. C. Lin, Y. Zhang, and S. Li, "Distributed *k*-Winners-Take-All With Privacy Protection: Method and Hardware Experiments," *IEEE Transactions on Industrial Electronics* 73, no. 9 (2026): 13663–13673, https://doi.org/10.1109/TIE.2026.3675190.

14. S. Liu and J. Wang, "A New *k*-Winners-Take-All Neural Network," in *Proceedings of the International Joint Conference on Neural Networks* (IEEE, 2005), 712–716.

15. Z. Zeng, J. Wang, and X. Liao, "IEEE Transactions on Circuits and Systems I: Fundamental Theory and Applications," *IEEE Transactions*

on Circuits and Systems I: Fundamental Theory and Applications 50, no. 10 (October 2003): 1353–1358, https://doi.org/10.1109/TCSI.

16. H. Huang, L. Jin, and Z. Zeng, "A Momentum Recurrent Neural Network for Sparse Motion Planning of Redundant Manipulators With Majorization-Minimization," *IEEE Transactions on Industrial Electronics* 72, no. 12 (December 2025): 13532–13541, https://doi.org/10.1109/tie.2025.3566731.

17. M. Liu, L. Chen, X. Du, L. Jin, and M. Shang, "Activated Gradients for Deep Neural Networks," *IEEE Transactions on Neural Networks and Learning Systems* 34, no. 4 (April 2023): 2156–2168, https://doi.org/10.1109/tnnls.2021.3106044.

18. Y. Chen, W. Du, H. Cao, and L. Jin, "Coevolutionary Neural Dynamics With Learnable Parameters for Nonconvex Optimisation," *CAAI Transactions on Intelligence Technology* 11, no. 1 (February 2026): 111–122, https://doi.org/10.1049/cit2.70074.

19. D. Ma, J. Zhang, L. Jin, and S. Li, "Discrete Neural Dynamics Combined With Kalman Filter for Cooperative Control of Multi-Robot Systems With Constraints," *IEEE Transactions on Control Systems Technology* 34, no. 4 (2026): 1954–1963, https://doi.org/10.1109/TCST.2026.3682333.

20. Y. Kong, S. Sun, Y. Jiang, and L. Wei, "Convergent Interval Confirmation for Three-Step Discrete Specific Zeroing Neural Dynamics Illustrated With Repetitive Motion Planning of Redundant Manipulators," *CAAI Transactions on Intelligence Technology* (2026): cit2.70126, https://doi.org/10.1049/cit2.70126.

21. J. Fan, L. Jin, P. Li, J. Liu, Z.-G. Wu, and W. Chen, "Coevolutionary Neural Dynamics Considering Multiple Strategies for Nonconvex Optimization," *Tsinghua Science and Technology* (2025), https://doi.org/10.26599/TST.2025.9010120.

22. J. Sum, C.-S. Leung, and K. I.-J. Ho, "On Wang *k*WTA With Input Noise, Output Node Stochastic, and Recurrent State Noise," *IEEE Transactions on Neural Networks and Learning Systems* 29, no. 9 (September 2018): 4212–4222, https://doi.org/10.1109/tnnls.2017.2759905.

23. W. Lu, Y. Zheng, and C.-S. Leung, "Effect of Time-Varying Multiplicative Noise on DNN-*k*WTA Model," *IEEE Transactions on Neural Networks and Learning Systems* 35, no. 12 (December 2024): 18922–18930, https://doi.org/10.1109/tnnls.2023.3317135.

24. H. Huang, W. He, and Z. Zeng, "An Integral-Enhanced Adaptive Gradient Neural Network for *k*WTA and Multirobot Coordination," *IEEE Transactions on Cybernetics* 56, no. 6 (June 2026): 3165–3176, https://doi.org/10.1109/tcyb.2025.3650634.

25. M. Liu, X. Zhang, M. Shang, and L. Jin, "Gradient-Based Differential *k*WTA Network With Application to Competitive Coordination of Multiple Robots," *IEEE/CAA Journal of Automatica Sinica* 9, no. 8 (August 2022): 1452–1463, https://doi.org/10.1109/jas.2022.105731.

26. J. Li, Y. Cao, Z. Xie, and L. Jin, "A *k*-Winners-Take-All (*k*WTA) Network With Noise Characteristics Captured," *IEEE/CAA Journal of Automatica Sinica* 12, no. 4 (April 2025): 734–744, https://doi.org/10.1109/jas.2025.125153.

27. X. Wang, S. Yang, Z. Guo, Q. Ge, S. Wen, and T. Huang, "A Distributed *k*-Winners-Take-All Model With Binary Consensus Protocols," *IEEE Transactions on Cybernetics* 54, no. 5 (May 2024): 3327–3337, https://doi.org/10.1109/tcyb.2023.3328716.

28. P. Duan, J. Qian, Q. Wang, Z. Duan, and L. Shi, "Distributed State Estimation for Continuous-Time Linear Systems With Correlated Measurement Noise," *IEEE Transactions on Automatic Control* 67, no. 9 (September 2022): 4614–4628, https://doi.org/10.1109/tac.2022.3165425.

29. Y. Wang, L. Zheng, and Y. Cai, "Multi-Class Hierarchical Random Networks for Consensus-Based Information Filter," *IEEE Transactions on Circuits and Systems I: Regular Papers* 72, no. 9 (September 2025): 4981–4993, https://doi.org/10.1109/tcsi.2024.3516371.

30. H. Yang and Y. Wang, "Finite-Gain Based Prescribed-Time Consensus Control for Multi-Agent Systems Under Switching Topology," *Automatica* 183 (January 2026): 112686, https://doi.org/10.1016/j.automatica.2025.112686.

31. S. Liang and L. Jin, "Distributed *k*-Winner-Take-All Network Under Weight-Unbalanced Topology," *IEEE Transactions on Circuits and Systems II: Express Briefs* 71, no. 2 (February 2024): 717–721, https://doi.org/10.1109/tcsii.2023.3306732.

32. L. Jin, Y. Qi, X. Luo, S. Li, and M. Shang, "Distributed Competition of Multi-Robot Coordination Under Variable and Switching Topologies," *IEEE Transactions on Automation Science and Engineering* 19, no. 4 (October 2022): 3575–3586, https://doi.org/10.1109/tase.2021.3126385.

33. Z. Wang and L. Xie, "Consensus for Multiagent Systems With Input Delay and Observation Packet Loss," *IEEE Transactions on Automatic Control* 70, no. 5 (May 2025): 3494–3501, https://doi.org/10.1109/tac.2024.3525257.

34. Y. Lv, H. Zhang, Z. Wang, and H. Yan, "Distributed Localization for Multi-Agent Systems With Random Noise Based on Iterative Learning," *IEEE Transactions on Neural Networks and Learning Systems* 35, no. 1 (January 2024): 952–960, https://doi.org/10.1109/tnnls.2022.3178077.

35. L. A. Badran, K. Ayrankia, and R. R. Selmic, "Stability and Convergence Analysis of Multi-Agent Consensus With Communication Delays: A Lambert W Function Approach," *IEEE Control Systems Letters* 9 (June 2025): 781–786, https://doi.org/10.1109/lcsys.2025.3578272.

36. X. Ma, D. Ma, and M. Liu, "Distribution-Allowed Noise-Resistant Neural Dynamics for Constrained Time-Dependent Quadratic Programming With *k*WTA Application," *IEEE Transactions on Systems, Man, and Cybernetics: Systems* 55, no. 5 (May 2025): 3732–3741, https://doi.org/10.1109/tsmc.2025.3547387.

37. L. Jin, S. Liang, X. Luo, and M. Zhou, "Distributed and Time-Delayed *k*-Winner-Take-All Network for Competitive Coordination of Multiple Robots," *IEEE Transactions on Cybernetics* 53, no. 1 (January 2023): 641–652, https://doi.org/10.1109/tcyb.2022.3159367.

38. K. Liu and Y. Zhang, "Distributed Dynamic Task Allocation for Moving Target Tracking of Networked Mobile Robots Using *k*-WTA Network," *IEEE Transactions on Neural Networks and Learning Systems* 36, no. 3 (March 2025): 5795–5802, https://doi.org/10.1109/tnnls.2024.3377433.

39. J. Kang, Y. Yuan, J. Shan, and M. Ryll, "Matrix-Weighted Coupling-Enhanced Adaptive Tracking Control for a Quadrotor-Slung-Load System," *IEEE Transactions on Industrial Electronics* 73, no. 6 (Junuary 2026): 8958–8969, https://doi.org/10.1109/tie.2026.3654765.

40. M. Liu, Y. Li, Y. Chen, Y. Qi, and L. Jin, "A Distributed Competitive and Collaborative Coordination for Multirobot Systems," *IEEE Transactions on Mobile Computing* 23, no. 12 (December 2024): 11436–11448, https://doi.org/10.1109/tmc.2024.3397242.